JOURNAL OF MECHANICAL ENGINEERING AND SCIENCES (JMES)
ISSN: 2289-4659 e-ISSN: 2231-8380
VOL. 16, ISSUE 1, 8706 – 8717
DOI: https://doi.org/10.15282/jmes.16.1.2022.05.0688

ORIGINAL ARTICLE

# Free vibration analysis of multi-layer rectangular plate containing magnetorheological fluid and flexible core layers rested on Winkler-Pasternak foundation

M. Shekarzadeh[1], M.M. Najafizadeh[1,*], P. Yousefi[1], A. Nezamabadi[1], K. Khorshidi[1,2]

[1] Department of Mechanical Engineering, Arak Branch, Islamic Azad University, 38135-567, Arak, Iran
[2] Mechanical Engineering Department, Faculty of Engineering, Arak University, 3848177584, Arak, Iran

**ABSTRACT** – Magneto-rheological (MR) fluids viscosity can be varied by changing the magnetic field intensity. Therefore, they can improve structural rigidity and damping property. The current study presents a free vibration analysis of a multilayer rectangular plate with two layers of MR fluid and a flexible core layer, rested on a Winkler-Pasternak foundation based on exponential shear deformation theory (ESDT). In this theory, the exponential functions are applied in terms of thickness coordinates to include the effect of transverse and inertial rotational shear deformation. The flexible core displacement is modeled via the second-order Frostig model. The Hamilton's principle is used to derive the equations of motion. These equations are solved using the Navier method to obtain the natural frequencies of the plate. The accuracy of the derived equations is validated, and the obtained results are compared with a specific case. Finally, the results show that by applying and increasing the magnetic field intensity, the natural frequencies and loss factor increase. With the increase in the mode number for each specific magnetic field intensity, the natural frequency increases and the loss factor decreases. The natural frequencies and loss factor decrease with the increase of the MR layer thickness to overall thickness ratio and the flexible core layer thickness to overall thickness ratio. The natural frequencies increase when the parameters of the foundation increase.

**ARTICLE HISTORY**
Received: 01st June 2020
Revised: 21st Jan 2022
Accepted: 24th Jan. 2022

**KEYWORDS**
*Vibration;*
*Magneto-rheological fluid plate;*
*exponential shear deformation theory;*
*Winkler-Pasternak foundation*

## INTRODUCTION

Although the plates have been studied from various aspects such as vibration, stability, etc., they are still a controversial topic for new studies [1]. The sandwich structures have been broadly used in many engineering fields such as transport, civil construction, marine and aerospace because these structures contain advantageous features (e.g. high strength to weight ratio and low maintenance cost). Given this, studying the behavior of these structures is very important to predict accurately critical loads and natural frequencies [2, 3]. In addition, they play a key role in controlling the vibration of structures. Since it is vital to achieving a way to control the vibration with higher efficiency and short time response, some of the researches notice the use of multilayer structures with smart fluids layer or flexible core or a combination of them. The smart fluids such as electro-rheological (ER) and magneto-rheological (MR) fluids have controllable rheology [4, 5].

The excellence of MR fluids on ER fluids is that they have more significant changes in their characteristics. Magneto-rheological fluids are a mixture of tiny magnetic particles in a carrier liquid. They alter rapidly from a liquid to a nearly solid state when in presence of a magnetic field [6] because magnetic particles are arranged in the direction of the magnetic field and give rise to a chain-like structure [7, 8]. Therefore, their yield stress changes over a few milliseconds as the magnetic field intensity changes [9, 10]. Sandwich structures coupled with controllable magnetic field yield continually vary stiffness and damping properties, and thereby could provide enhanced vibration isolation in a wide frequency range. Due to its outstanding features, various high-performance MR fluid devices have been designed and tested [11-17].

According to reported researches, it is found that the sandwich structures have been studied from different aspects which illustrate the following. Yeh and Shih [18] analyzed the dynamic features and instability of the structures containing magneto-rheological fluid under buckling loads. Rajamohan et al. [19] derived the formulations for a sandwich beam with a magneto-rheological fluid layer, and presented their validity via experiments on a cantilever sandwich beam. It was indicated that the natural frequencies rise with an increase in the magnetic field. Mohammadi and Sedaghati [20], investigated the nonlinear vibration behavior of sandwich shell structures with a constrained ER fluid.

Yeh [21] studied the vibration of the sandwich plate with a magneto-rheological fluid core by the FEM method. Rajamohan et al.[10] studied the dynamic features of a sandwich beam with the magneto-rheological fluid internal core between the two layers of the continuous elastic structure. Yeh [22], investigated the vibration features of an orthotropic sandwich plate with a rectangular shape and magneto-rheological fluid core and constraining layer.

*CORRESPONDING AUTHOR | M.M. Najafizadeh | ✉ m-najafizadeh@iau-arak.ac.ir

Hoseinzadeh and Rezaeepazhand [23], studied the dynamic behavior of composite laminated plates under the influence of external ER dampers. Eshaghi et al. [24], studied analytical and experimental free vibration of sandwich annular circular plates comprising the magneto-rheological fluid core. Payganeh et al. [25] studied the free vibration of sandwich panels with flexible core and magneto-rheological fluid layers. Eshaghi et al. [26], investigated the free vibration of a cantilevered sandwich plate partially treated with a magneto-rheological fluid core. Arani and Soleymani [27], studied a size-dependent vibration analysis of a rotating MR doubly-tapered sandwich beam in supersonic airflow.

The analysis of elastic foundations is required in applications such as, roads, airports, building foundations, docks, tanks and more structures. Winkler presented a linear one-parameter model for the force and energy of an elastic foundation for the first time. In this model, the foundation reaction force is assumed to be a proportional relationship between pressure and deflection of the foundation. Winkler model is simulated with the normal springs and does not consider shear deformations [28]. Pasternak presented a two-parameter model to describe the foundation behavior. This model consider shear deformation in addition to normal deformation [29]. It is widely accepted to describe the mechanical behavior of the foundations.

Huang et al. [30], investigated the exact solution of FGM thick plate resting on the winkler-pasternak foundation. Atman et al. [31], studied the vibration of FGM plates resting on the winkler-pasternak foundation using new shear deformation theory.

Here, the free vibration of a sandwich panel with a flexible core and magneto-rheological fluid layers is studied. The displacement of the core is modeled using Frostig's second-order model. In this model, the displacement is thought to be in the form of a polynomial with unknown coefficients. The displacement of the sheets is modeled via ESDT. In this theory, as in theory used by Benferhat et al.[32], there is no need for shear correction factors compared to first-order shear deformation theory. The studied plate is rested on a Winkler-Pasternak foundation. Hamilton's principle is used to obtain motion equations. The simple support for all edges are considered as boundary conditions. Derived equations are solved via the Navier method.

## THEORETICAL FORMULATION

The studied sandwich panel is shown in Figure 1. It is a rectangular panel that it's length, width and thickness are named with $a$, $b$ and $h$, respectively. It has a flexible foam core that is denoted by '$c$' index in this text. There are two sets at both top and bottom of the flexible core. Each set contains an enclosed MR layer by two composite sheets. The '$t$' and '$b$' indices are used for upper and lower layers, respectively. Additionally, the '*1*' index is used for face composite sheets, similarly '*2*' for MR layers and '3' for the nearest layers to the flexible core.

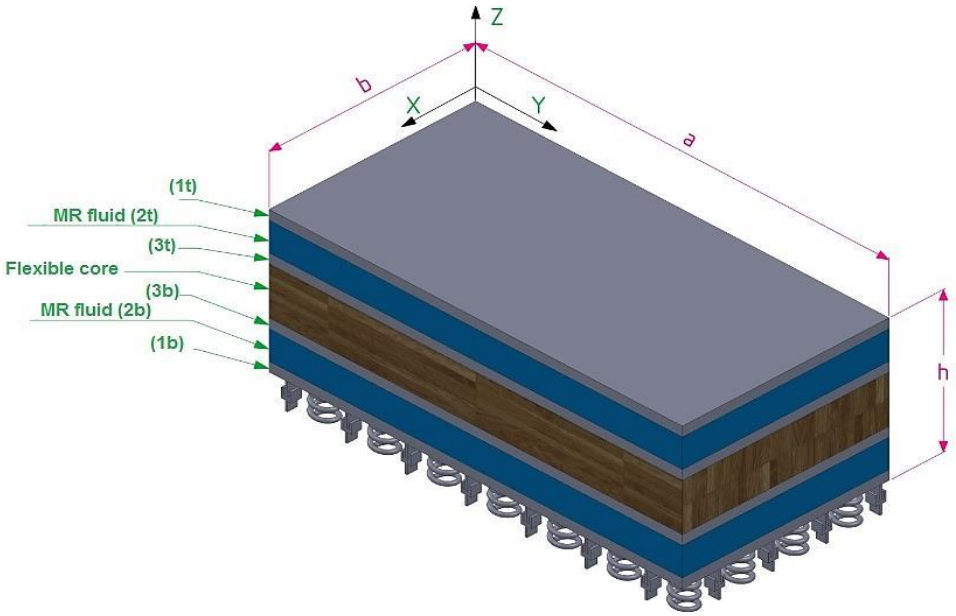


**Figure 1.** Schematics of the sandwich plate with two MR fluid layers and a flexible core resting on elastic foundation

### Displacement and Strain Fields

The displacement field of the face sheets is modeled by exponential shear deformation theory shown below [33]:

$$u_i(x,y,z,t) = u_0^i(x,y,t) - z\frac{\partial w_0^i(x,y,t)}{\partial x} + f(z_i)\varphi^i(x,y,t) \tag{1a}$$

$$v_i(x,y,z,t) = v_0^i(x,y,t) - z\frac{\partial w_0^i(x,y,t)}{\partial y} + f(z_i)\psi^i(x,y,t) \tag{1b}$$

$$w_i(x,y,z,t) = w_0^i(x,y,t) \tag{1c}$$

Where $i = 1t, 3t, 3b, 1b$ and $f(z_i) = z_i\left(e^{-2\left(\frac{z_i}{h_i}\right)^2}\right)$. Also, $u_i$, $v_i$ and $w_i$ are displacements in the $x$, $y$ and $z$ directions, respectively. The mid-plane displacements are shown by $u_0^i$, $v_0^i$ and $w_0^i$. $\varphi^i$ and $\psi^i$ are the rotation functions along the $x$ and $y$ axes, respectively. Unlike the FSDT method, this theory does not require the use of shear correction factors, similarly the used theory in [32]. According to the Frostig's second model, the displacement field for the flexible core is as below [34]:

$$u_c(x,y,z,t) = u_0^c(x,y,t) + z_c u_1^c(x,y,t) + z_c^2 u_2^c(x,y,t) + z_c^3 u_3^c(x,y,t) \tag{2a}$$

$$v_c(x,y,z,t) = v_0^c(x,y,t) + z_c v_1^c(x,y,t) + z_c^2 v_2^c(x,y,t) + z_c^3 v_3^c(x,y,t) \tag{2b}$$

$$w_c(x,y,z,t) = w_0^c(x,y,t) + z_c w_1^c(x,y,t) + z_c^2 w_2^c(x,y,t \tag{2c}$$

The linear strains in the upper and lower sheets ($i = 1t, 3t, 3b, 1b$) based on Von-Karman strain assumptions are as below [35]:

$$\varepsilon_{xx}^i = u_{0,x}^i - z_i w_{0,xx}^i + f(z_i)\varphi_{,x}^i \tag{3a}$$

$$\varepsilon_{yy}^i = v_{0,y}^i - z_i w_{0,yy}^i + f(z_i)\psi_{,y}^i \tag{3b}$$

$$\gamma_{xy}^i = 2\varepsilon_{xy}^i = u_{0,y}^i + v_{0,x}^i - 2z_i w_{0,xy}^i + f(z_i)\varphi_{,y}^i + f(z_i)\psi_{,x}^i \tag{3c}$$

$$\gamma_{xz}^i = 2\varepsilon_{xz}^i = \frac{df(z_i)}{dz}\varphi^i \tag{3d}$$

$$\gamma_{yz}^i = 2\varepsilon_{yz}^i = \frac{df(z_i)}{dz}\psi^i \tag{3e}$$

Also the linear strains in the core layer based on Von-Karman strain assumptions are as below [35]:

$$\varepsilon_{xx}^c = u_{0,x} + z_c u_{1,x} + z_c^2 u_{2,x} + z_c^3 u_{3,x} \tag{4a}$$

$$\varepsilon_{yy}^c = v_{0,y} + z_c v_{1,y} + z_c^2 v_{2,y} + z_c^3 v_{3,y} \tag{4b}$$

$$\varepsilon_{zz}^c = w_1 + 2z_c w_2 \tag{4c}$$

$$\gamma_{xy}^c = u_{0,y} + z_c u_{1,y} + z_c^2 u_{2,y} + z_c^3 u_{3,y} + v_{0,x} + z_c v_{1,x} + z_c^2 v_{2,x} + z_c^3 v_{3,x} \tag{4d}$$

$$\gamma_{xz}^c = u_1 + 2z_c u_2 + 3z_c^2 u_3 + w_{0,x} + z_c w_{1,x} + z_c^2 w_{2,x} \tag{4e}$$

$$\gamma_{yz}^c = v_1 + 2z_c v_2 + 3z_c^2 v_3 + w_{0,y} + z_c w_{1,y} + z_c^2 w_{2,y} \tag{4f}$$

## Relations of Magnetorheological Layer

The relationship between transverse strains and stresses in MR layers can be expressed as:

$$\tau_{xz}^{2j} = G^*\gamma_{xz}^{2j} \qquad (j = t, b) \tag{5a}$$

$$\tau_{yz}^{2j} = G^*\gamma_{yz}^{2j} \qquad (j = t, b) \tag{5b}$$

According to the geometrical relationships between displacement components and rotation functions in layers 1 and 3, and also the assumption that a no-slip condition exists between sheet layers and magnetorheological fluid layers, the components of strain in MR layers can be given as:

$$\gamma_{xz}^{2j} = \frac{\partial w_j}{\partial x} + \frac{u_0^{1j} - u_0^{3j}}{h_{2j}} + \frac{\partial w_j}{\partial x}\frac{h_{1j} + h_{3j}}{2h_{2j}} + \frac{\varphi^j}{2h_{2j}}\left(h_{2j}e^{-2\left(\frac{h_{1j}}{2h_{2j}}\right)^2} - h_{2j}e^{-2\left(\frac{h_{3j}}{2h_{2j}}\right)^2}\right) \tag{6a}$$

$$\gamma_{yz}^{2j} = \frac{\partial w_j}{\partial y} + \frac{v_0^{1j} - v_0^{3j}}{h_{2j}} + \frac{\partial w_j}{\partial y}\frac{h_{1j} + h_{3j}}{2h_{2j}} + \frac{\psi^j}{2h_{2j}}\left(h_{2j}e^{-2\left(\frac{h_{1j}}{2h_{2j}}\right)^2} - h_{2j}e^{-2\left(\frac{h_{3j}}{2h_{2j}}\right)^2}\right) \tag{6b}$$

The magnetorheological fluid shows the viscoelastic behavior in the pre-yield range, that is described in terms of the complex modulus $G^*$.

$$G^* = G' + iG'' \tag{7}$$

Here, $G'$ and $G''$ are the storage modulus and the loss modulus, respectively. They are described as [25]:

$$G' = -3.3691B^2 + 4.9975 \times 10^3 B + O.893 \times 10^6 \tag{8a}$$

$$G'' = -0.9B^2 + 0.8124 \times 10^3 B + O.1855 \times 10^6 \tag{8b}$$

Here, $B$ represents the magnetic field intensity in Gauss.

### Relations of the Foundation

The two parameter Winkler-Pasternak model is used to model the elastic foundation. This model considers transvers shear deformations in addition to vertical deformations. In this model, the elastic foundation reaction force per unit of area is introduced as:

$$f_e = k_w w - k_{gx}\frac{\partial^2 w}{\partial x^2} - k_{gy}\frac{\partial^2 w}{\partial y^2} \tag{9}$$

Where $k_w$ , $k_{gx}$ and $k_{gy}$ are dimensionless parameters of the elastic foundation which in isotropic foundations, $k_{gx} = k_{gy}$. Since the foundation is in contact with the bottom layer, the vertical displacement of this layer affects the foundation. So, the strain energy of the elastic foundation is considered as:

$$U_f = \int f_e w_b ds \tag{10}$$

## EQUATIONS OF MOTION

To extract the equations of motion, the Hamilton's principle is employed as below:

$$\int_{t_1}^{t_2} (\delta U + \delta V - \delta T + U_f) = 0 \tag{11}$$

Where $\delta$, $U$, $V$, $T$ and $U_f$ are the variation operator, the strain energy, the work done by external forces, the kinetic energy and the elastic foundation energy, respectively. In the current research, $V$ is zero, and:

$$\begin{aligned}\delta U = &\sum_{i=1t,3t,3b,1b}\left\{\int_{v_i}(\sigma_{xx}^i\delta\varepsilon_{xx}^i + \sigma_{yy}^i\delta\varepsilon_{yy}^i + \tau_{xy}^i\delta\gamma_{xy}^i + \tau_{xz}^i\delta\gamma_{xz}^i + \tau_{yz}^i\delta\gamma_{yz}^i)dv_i\right\} \\ &+ \sum_{i=2t,2b}\left\{\int_{v_i}(\tau_{xz}^i\delta\gamma_{xz}^i + \tau_{yz}^i\delta\gamma_{yz}^i)dv_i\right\} \\ &+ \int_{v_c}(\sigma_{zz}^c\delta\varepsilon_{zz}^c + \tau_{xz}^c\delta\gamma_{xz}^c + \tau_{yz}^c\delta\gamma_{yz}^c + \sigma_{xx}^c\delta\varepsilon_{xx}^c + \sigma_{yy}^c\delta\varepsilon_{yy}^c + \tau_{xy}^c\delta\gamma_{xy}^c)dv_c\end{aligned} \tag{12}$$

$$\delta T = -\sum_{i=1t,3t,3b,1b}\left\{\int_0^a\int_0^b \rho_i\, h_i(\dot{u}_i\delta\dot{u}_i + \dot{v}_i\delta\dot{v}_i + \dot{w}_i\delta\dot{w}_i)dxdy\right\}$$
$$-\sum_{i=2t,2b}\left\{\int_0^a\int_0^b \left(\rho_j h_j \dot{w}_j\delta\dot{w}_j + I_{MR}\left(\dot{\gamma}_{xz}^j\delta\dot{\gamma}_{xz}^j + \dot{\gamma}_{yz}^j\delta\dot{\gamma}_{yz}^j\right)\right)dxdy\right\} \quad (13)$$
$$-\int_0^a\int_0^b \rho_c\, h_c(\dot{u}_c\delta\dot{u}_c + \dot{v}_c\delta\dot{v}_c + \dot{w}_c\delta\dot{w}_c)dxdy$$

Where, $\rho$ is the mass density, dot-over script convention index illustrates the derivation of variables over time. Also, it is assumed that there is no normal stress in MR layers ($2t$ and $2b$). By using Eq. (11) and considering the stress resultants, forces and momentums which are defined in Eqs. (14a)-(14i), the equations of motion are derived.

$$\{N_{xx}^i, N_{yy}^i, N_{xy}^i, Q_{xz}^i, Q_{yz}^i\} = \int_{-\frac{h_i}{2}}^{\frac{h_i}{2}} \{\sigma_{xx}^i, \sigma_{yy}^i, \tau_{xy}^i, \tau_{xz}^i, \tau_{yz}^i\}dz_i \qquad (i = 1t, 3t, 1b, 3b, c) \quad (14a)$$

$$\{M_{xx}^i, M_{yy}^i, M_{xy}^i\} = \int_{-\frac{h_i}{2}}^{\frac{h_i}{2}} z_i\{\sigma_{xx}^i, \sigma_{yy}^i, \tau_{xy}^i\}dz_i \qquad (i = 1t, 3t, 1b, 3b) \quad (14b)$$

$$\{M_{nxx}^c, M_{nyy}^c, M_{nxy}^c, M_{Qnxz}^c, M_{Qnyz}^c\} = \int_{-\frac{h_i}{2}}^{\frac{h_i}{2}} z_c^n\{\sigma_{xx}^c, \sigma_{yy}^c, \tau_{xy}^c, \tau_{xz}^c, \tau_{yz}^c\}dz_c \quad (14c)$$

$$\{R_z^c, M_z^c\} = \int_{-\frac{h_i}{2}}^{\frac{h_i}{2}} \{1, z_c\}\sigma_{zz}^c dz_c \quad (14d)$$

$$\{Q_{xz}^i, Q_{yz}^i\} = \int_{-\frac{h_i}{2}}^{\frac{h_i}{2}} \{\tau_{xz}^i, \tau_{yz}^i\}dz_i \qquad (i = 2t, 2b) \quad (14e)$$

$$I_n^i = \int_{-\frac{h_i}{2}}^{\frac{h_i}{2}} z_i^n \rho_i dz_i \qquad i = c, 1t, 3t, 1b, 3b \qquad n = 0,1,2,\ldots \quad (14f)$$

$$\{J_0^i, J_1^i, J_2^i\} = \int_{-\frac{h_i}{2}}^{\frac{h_i}{2}} \rho_i\{f(z_i), z_i f(z_i), (f(z_i))^2\}dz_i \qquad i = 1t, 3t, 1b, 3b \quad (14g)$$

$$\{R_{xx}^i, R_{yy}^i, R_{xy}^i\} = \int_{-\frac{h_i}{2}}^{\frac{h_i}{2}} \{\sigma_{xx}^i, \sigma_{yy}^i, \tau_{xy}^i\}f(z_i)dz_i \qquad i = 1t, 3t, 1b, 3b \quad (14h)$$

$$\{P_x^i, P_y^i\} = \int_{-\frac{h_i}{2}}^{\frac{h_i}{2}} \{\tau_{xz}^i, \tau_{yz}^i\}\frac{df(z_i)}{dz_i}\, dz_i \qquad i = 1t, 3t, 1b, 3b \quad (14i)$$

Since the derived equations of motion are too long, they are presented only for layer "1t" in Eqs. (15a)-(15c). The other layers have the same equations approximately, that aren't presented here.

$$\delta u_o^{1t}:$$

$$N_{xx,x}^{1t} + N_{xy,y}^{1t} + \frac{1}{h_{2t}} Q_{xz}^{2t} - I_o^{1t}\ddot{u}_0^{1t} + I_1^{1t}\ddot{w}_{0,x}^{t} - J_0^{1t}\ddot{\varphi}^{t} + \frac{h_{1t}+h_{3t}}{2h_{2t}^2} I_o^{2t}\ddot{\varphi}^{t} - \frac{1}{h_{2t}^2} I_o^{2t}\ddot{u}_0^{1t} + \frac{1}{h_{2t}^2} I_o^{2t}\ddot{u}_0^{3t} - \frac{1}{h_{2t}} I_o^{2t}\ddot{w}_{0,x}^{t} = 0 \tag{15a}$$

$$\delta v_o^{1t}:$$

$$N_{yy,y}^{1t} + N_{xy,x}^{1t} + \frac{1}{h_{2t}} Q_{yz}^{2t} - I_0^{1t}\ddot{v}_0^{1t} + I_1^{1t}\ddot{w}_{0,y}^{t} - J_0^{1t}\ddot{\psi}^{t} + \frac{h_{1t}+h_{3t}}{2h_{2t}^2} I_o^{2t}\ddot{\psi}^{t} - \frac{1}{h_{2t}^2} I_o^{2t}\ddot{v}_0^{1t} + \frac{1}{h_{2t}^2} I_o^{2t}\ddot{v}_0^{3t} - \frac{1}{h_{2t}} I_o^{2t}\ddot{w}_{0,y}^{t} = 0 \tag{15b}$$

$$\delta w_0^{1t}:$$

$$\begin{aligned}
&M_{xx,xx}^{1t} + M_{xx,xx}^{3t} + M_{xy,xy}^{1t} + M_{xy,xx}^{3t} + +M_{yy,yy}^{1t} + +M_{yy,yy}^{3t} - \frac{h_{3t}}{h_c^2} M_{2xx,xx}^{c} - \frac{2h_{3t}}{h_c^3} M_{3xx,xx}^{c} - \frac{h_{3t}}{h_c^2} M_{2yy,yy}^{c} - \frac{2h_{3t}}{h_c^3} M_{3yy,yy}^{c} + \\
&\frac{1}{h_c} R_z^c + \frac{4}{h_c^2} M_z^c - \frac{4h_{3t}}{h_c^3} M_{3xy,xy}^{c} + (\frac{2h_{3t}}{h_c^2} + \frac{1}{h_c}) M_{Q1xz,x}^{c} + (\frac{6h_{3t}}{h_c^3} + \frac{2}{h_c^2}) M_{Q2xz,x}^{c} + (\frac{2h_{3t}}{h_c^2} + \frac{1}{h_c}) M_{Q1yz,y}^{c} + (\frac{6h_{3t}}{h_c^3} + \frac{2}{h_c^2}) M_{Q2yz,y}^{c} + \\
&Q_{xz,x}^{2t} + Q_{yz,y}^{2t} + I_1^{1t}\ddot{u}_{0,x}^{1t} + \left(I_1^{3t} - \frac{8h_{3t}I_6^c}{h_c^6} - \frac{8h_{3t}I_5^c}{h_c^5} - \frac{2h_{3t}I_4^c}{h_c^4}\right)\ddot{u}_{0,x}^{3t} + \left(\frac{8h_{3t}I_6^c}{h_c^6} - \frac{2h_{3t}I_4^c}{h_c^4}\right)(\ddot{u}_{0,x}^{3b} + \ddot{v}_{0,y}^{3b}) + \left(-I_2^{1t} - I_2^{3t} - \frac{4h_{3t}^2I_6^c}{h_c^6} - \right. \\
&\left. \frac{4h_{3t}^2I_5^c}{h_c^5} + \frac{h_{3t}h_{3b}I_4^c}{h_c^4} - \frac{h_{3t}^2I_4^c}{h_c^4}\right)\ddot{w}_{0,xx}^{t} + \left(-\frac{4h_{3t}h_{3b}I_6^c}{h_c^6} + \frac{h_{3t}h_{3b}I_4^c}{h_c^4}\right)(\ddot{w}_{0,xx}^{b} + \ddot{w}_{0,yy}^{b}) + \left(-I_2^{1t} - I_2^{3t} - \frac{4h_{3t}^2I_6^c}{h_c^6} - \frac{4h_{3t}^2I_5^c}{h_c^5} - \frac{h_{3t}^2I_4^c}{h_c^4}\right)\ddot{w}_{0,yy}^{t} + \\
&\left(J_1^{1t} + J_1^{3t} + \frac{4h_{3t}^2I_6^c}{h_c^6}e^{-\frac{1}{2}} + \frac{4h_{3t}^2I_5^c}{h_c^5}e^{-\frac{1}{2}} + \frac{h_{3t}^2I_4^c}{h_c^4}e^{-\frac{1}{2}}\right)(\ddot{\varphi}_{,x}^{t} + \ddot{\psi}_{,y}^{t}) + \left(\frac{4h_{3t}h_{3b}I_6^c}{h_c^6}e^{-\frac{1}{2}} - \frac{h_{3t}h_{3b}I_4^c}{h_c^4}e^{-\frac{1}{2}}\right)(\ddot{\varphi}_{,x}^{b} + \ddot{\psi}_{,y}^{b}) + \\
&(-I_0^{1t} - I_0^{3t})\ddot{w}_0^t + I_1^{1t}\ddot{v}_{0,y}^{1t} + \left(I_1^{3t} - \frac{8h_{3t}I_6^c}{h_c^6} - \frac{8h_{3t}I_5^c}{h_c^5} - \frac{2h_{3t}I_4^c}{h_c^4}\right)\ddot{v}_{0,y}^{3t} + \left(\frac{8h_{3t}I_5^c}{h_c^5} + \frac{4h_{3t}I_4^c}{h_c^4} - \frac{2h_{3t}I_3^c}{h_c^3} - \frac{h_{3t}I_2^c}{h_c^2}\right)(\ddot{u}_{0,x}^{c} + \ddot{v}_{0,y}^{c}) + \\
&\left(\frac{8h_{3t}I_6^c}{h_c^5} + \frac{4h_{3t}I_5^c}{h_c^4} - \frac{2h_{3t}I_4^c}{h_c^3} - \frac{h_{3t}I_3^c}{h_c^2}\right)(\ddot{u}_{1,x}^{c} + \ddot{v}_{1,y}^{c}) + \left(-\frac{4I_4^c}{h_c^4} + \frac{I_2^c}{h_c^2}\right)\ddot{w}_0^b + \left(-\frac{4I_4^c}{h_c^4} + \frac{4I_3^c}{h_c^3} - \frac{I_2^c}{h_c^2}\right)\ddot{w}_0^t + \left(\frac{8I_4^c}{h_c^4} + \frac{4I_3^c}{h_c^3} - \frac{2I_2^c}{h_c^2} - \frac{I_1^c}{h_c}\right)\ddot{w}_0^c - \\
&I_0^{2t}\ddot{w}_0^t + \left(\frac{h_{1t}+h_{3t}}{2h_{2t}}\right)(I_0^{2t}\ddot{\varphi}_{,x}^{t} + I_0^{2t}\ddot{\psi}_{,y}^{t}) - \frac{1}{h_{2t}} I_0^{2t}\ddot{u}_{0,x}^{1t} + \frac{1}{h_{2t}} I_0^{2t}\ddot{u}_{0,x}^{3t} - I_0^{2t}\ddot{w}_{0,xx}^{t} - I_0^{2t}\ddot{w}_{0,yy}^{t} - \frac{1}{h_{2t}} I_0^{2t}\ddot{v}_{0,y}^{1t} + \frac{1}{h_{2t}} I_0^{2t}\ddot{v}_{0,x}^{3t} = 0
\end{aligned} \tag{15c}$$

## SOLUTION METHOD

The Navier technique has been used to solve the derived equations as below, considering simply supported boundary condition for all edges, [33]:

$$\begin{Bmatrix} u_0^{ij} \\ u_0^c \\ u_1^c \end{Bmatrix} = \sum_{n=1}^{\infty}\sum_{m=1}^{\infty} \begin{Bmatrix} u_{mn}^{ij} \\ u_{0mn}^c \\ u_{1mn}^c \end{Bmatrix} \cos\alpha x \ \sin\beta y \ e^{J\omega t} \tag{16a}$$

$$\begin{Bmatrix} v_0^{ij} \\ v_0^c \\ v_1^c \end{Bmatrix} = \sum_{n=1}^{\infty}\sum_{m=1}^{\infty} \begin{Bmatrix} v_{mn}^{ij} \\ v_{0mn}^c \\ v_{1mn}^c \end{Bmatrix} \sin\alpha x \ \cos\beta y \ e^{J\omega t} \tag{16b}$$

$$\begin{Bmatrix} w_0^j \\ w_0^c \end{Bmatrix} = \sum_{n=1}^{\infty}\sum_{m=1}^{\infty} \begin{Bmatrix} w_{mn}^j \\ w_{mn}^c \end{Bmatrix} \sin\alpha x \ \sin\beta y \ e^{J\omega t} \tag{16c}$$

$$\{\varphi^j\} = \sum_{n=1}^{\infty}\sum_{m=1}^{\infty} \{\varphi_{mn}^j\} \cos\alpha x \sin\beta y \, e^{J\omega t} \tag{16d}$$

$$\{\psi^j\} = \sum_{n=1}^{\infty}\sum_{m=1}^{\infty} \{\psi_{mn}^j\} \sin\alpha x \cos\beta y \, e^{J\omega t} \tag{16e}$$

In the Eqs. (16a) to (16e), $i = 1,3$ , $j = t, b$, $\alpha = \frac{n\pi}{a}$ and $\beta = \frac{m\pi}{b}$ . By substituting Eqs. (16a)-(16e) in derived equations of motion, the simplified equation of motion can be provided as follow:

$$\{[K] - [M]\omega^2\}[\Delta] = 0 \tag{17}$$

Where $K$, $M$ and $\Delta$ are the stiffness matrix, mass matrix and displacement vector, respectively and $\Delta$ can be defined as:

$$\{\Delta\} = \{u_{mn}^{1t}, u_{mn}^{1b}, u_{mn}^{3t}, u_{mn}^{3b}, v_{mn}^{1t}, v_{mn}^{1b}, v_{mn}^{3t}, v_{mn}^{3b}, w_{mn}^{t}, w_{mn}^{b}, \varphi_{mn}^{t}, \varphi_{mn}^{b}, \psi_{mn}^{t}, \psi_{mn}^{b}, u_{0mn}^{c}, u_{1mn}^{c}, v_{0mn}^{c}, v_{1mn}^{c}, w_{0mn}^{c}\}^T \tag{18}$$

To solve Eqs. (18), the determinant of $([K] - \omega^2[M])$ must be zero. The calculated eigenvalues of this equation are in the complex form. So, the natural frequencies, $\omega^*$ and modal loss factor, $\eta$, are calculated as follow:

$$\omega^* = \sqrt{(Re(\omega))^2 + (Im(\omega))^2} \tag{19}$$

$$\eta = \frac{Im(\omega)}{Re(\omega)} \tag{20}$$

## RESULTS AND DISCUSSION

The accuracy verification of the current approach relies on the comparison of the obtained natural frequencies of the panel in the present study with the results of reference [25]. For this purpose, the foundation is neglected and the mechanical and geometric properties of the panel are designated as Table 1 and Table 2.

**Table 1.** Mechanical properties of the sandwich panel [25]

| Property | $E_1\ (Gpa)$ | $E_2\ (Gpa)$ | $E_3\ (Gpa)$ | $G_{12}\ (Gpa)$ | $G_{13}\ (Gpa)$ | $G_{23}\ (Gpa)$ | $\vartheta_{12}$ | $\vartheta_{13}$ | $\vartheta_{23}$ | $\rho\ (kg/m^3$ |
|---|---|---|---|---|---|---|---|---|---|---|
| **Face Sheets** | 24.51 | 7.77 | 7.77 | 3.34 | 3.34 | 1.34 | 0.078 | 0.078 | 0.49 | 1800 |
| **Flexible Coree** | 0.1036 | 0.1036 | 0.1036 | 0.05 | 0.05 | 0.05 | 0.036 | 0.036 | 0.036 | 130 |

**Table 2.** Geometric properties of the sandwich panel [25]

| $h_{1t}\ (mm)$ | $h_{1b}\ (mm)$ | $h_{2t}\ (mm)$ | $h_{2b}\ (mm)$ | $h_{3t}\ (mm)$ | $h_{3b}\ (mm)$ | $h_c/h$ | $h/a$ |
|---|---|---|---|---|---|---|---|
| 1 | 1 | 1 | 1 | 2 | 2 | 0.88 | 0.1 |

To compare results of this method with reference [25], the density of used material in MR layer for a square sandwich panel, the magnetic field intensity and the arrangement of layers are considered as $\rho = 3500\ kg/m^3$ , B=150 Gauss and (0/90/MR/0/core/0/MR/90/0) respectively. Also four dimensionless frequencies are derived based on:

$$\overline{\omega} = \frac{\omega a^2}{h}\sqrt{\frac{\rho_c}{E_c}} \tag{21}$$

The results shown in Table 3 are close to the results of reference [25]. The reason for the difference between the results of the present study and reference [25] is the transverse shear stresses at the top and bottom surfaces of the plate are zero in ESDT while in FSDT, the correction factor is necessary because of the lack of control of shear stresses at the top and bottom surfaces of the plate. Therefore, it is concluded that the used theory can simulate the vibrational behavior of the plate better than FSDT.

**Table 3.** Comparison of dimensionless frequencies $\overline{\omega}$ between present study and reference [25]

| Mode number | (1,1) | (1,2) | (2,1) | (2,2) |
|---|---|---|---|---|
| **Reference [25]** | 20.54 | 13.72 | 33.22 | 23.31 |
| **Present study** | 18.75 | 12.69 | 32.55 | 20.51 |

### Effect of the Magnetic Field Intensity Variations on the Natural Frequency and Loss Factor

To examine the influence of the magnetic field intensity on the natural frequency and loss factor, a plate with presented properties in Tables 1 and 2, is considered. Also, the foundation parameters are; $k_w = 10^5$ and $k_g = 10^{15}$ . The results, in four modes of vibration, using Eqs. (19) and (20), are shown in Figure 2 and Figure 3. The increase in the magnetic field intensity causes the complex shear modulus of the magnetorhelogical fluid increases. Thus, the structure stiffness will increase. For this reason, it is observed from the results in Figure 2 that, the natural frequencies increase by applying and increasing the magnetic field intensity. Also, the results show that the larger mode number, the higher natural frequencies of the sandwich plate for each specific magnetic field intensity.

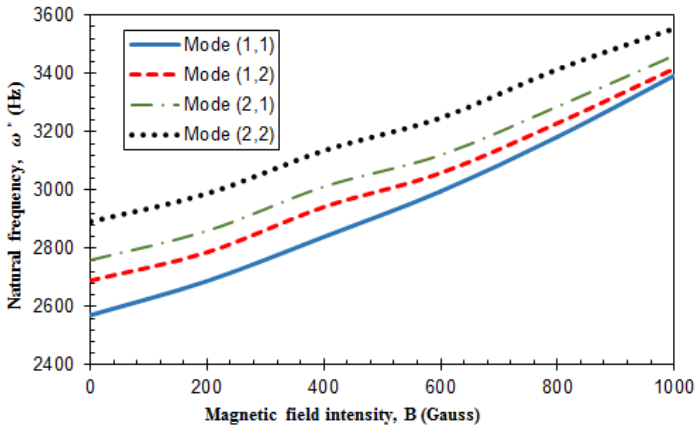


**Figure 2.** Effect of variations in the magnetic field intensity on the natural frequency

The variations in the loss factors for different magnetic field intensities are shown in Figure 3. It can be concluded that the loss factors increase with the increase in the magnetic field intensity. But this increase is greater at first, and as the magnetic field intensity increases, the increase in the loss factor will be smaller especially in the fundamental mode. Also, the loss factor decreases with the increase in the mode number for each specific magnetic field intensity.

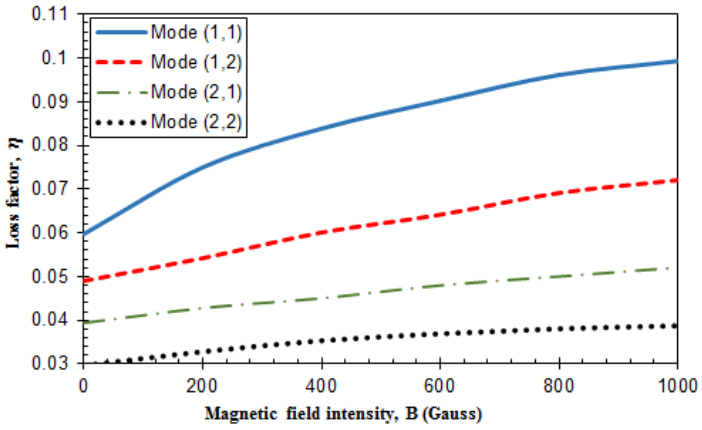


**Figure 3.** Effect of variations in the magnetic field intensity on the loss factor

### Effect of the Magnetorheological Fluid Layer Thickness on the Natural Frequency and Loss Factor

In Figure 4, the effect of the magnetorheological fluid layer thickness on the natural frequencies can be observed. The analysis conditions are similar to before section, except that the magnetic field intensity is considered 400 Guass. It is found when the MR layer thickness to overall thickness ratio increases, the natural frequencies decrease. It is attributed that the mass and stiffness of the structure both increase when the thickness of the MR layer increases, but increasing the mass of the structure is more than increasing the stiffness of the structure. Also it is observed the reduction in the natural frequencies is more significant in higher modes.

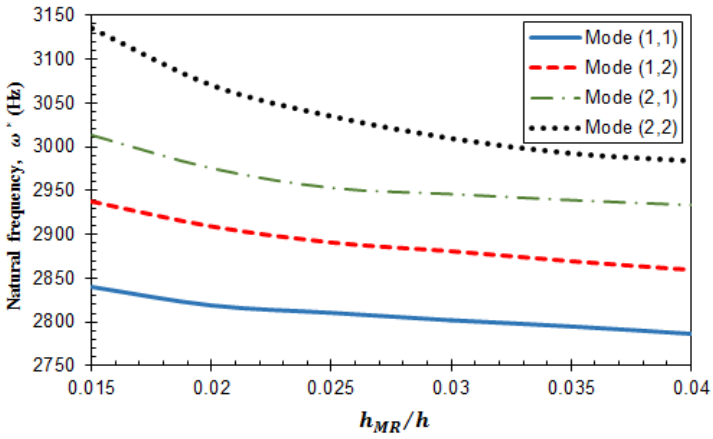


**Figure 4.** Effect of variations in the MR layer thickness to overall thickness ratio on the natural frequency

The effect of the magneto-rheological fluid layer thickness on the loss factors is shown in Figure 5. It is illustrated that the loss factors decrease with the increase of the MR layer thickness to overall thickness ratio. Also, the variations of the loss factors in higher modes are less than those compared to the lower modes.

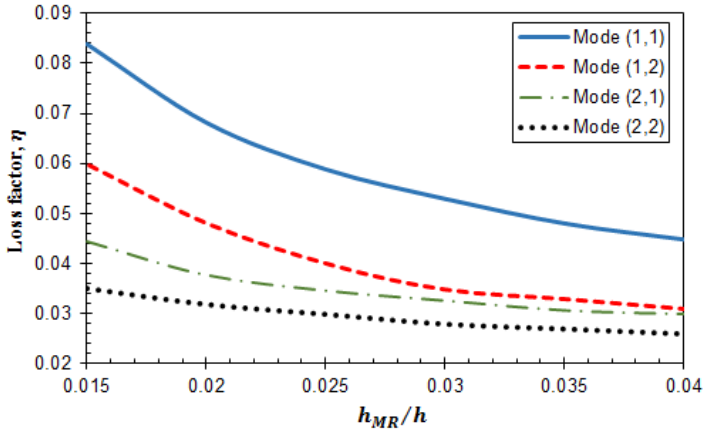


**Figure 5.** Effect of variations in the MR layer thickness to overall thickness ratio on the loss factor

## Effect of the Flexible Core Layer Thickness on the Natural Frequency and Loss Factor

The effect of the flexible core layer thickness on the natural frequencies is investigated at a magnetic field intensity of 400 Guass in Figure 6. The other analysis conditions are similar before section.

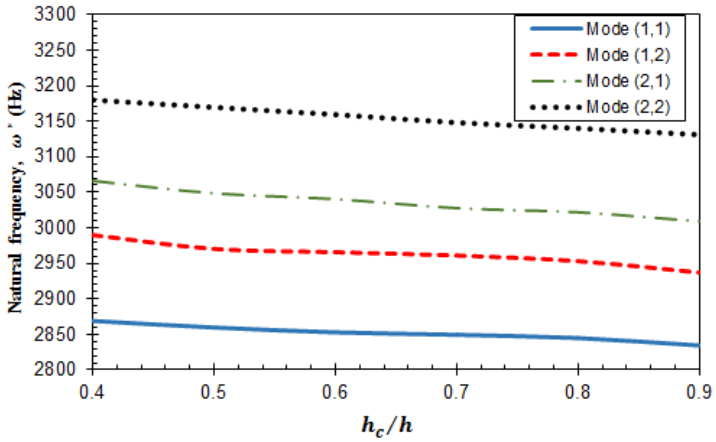


**Figure 6.** Effect of variations in the core layer thickness to overall thickness ratio on the natural frequency

It is observed that the natural frequencies decrease when the flexible core layer thickness to overall thickness ratio increases, but the range of this decrease in not large. It is attributed that the mass and stiffness of the structure both increase when the thickness of the flexible core layer increases, but increasing the mass of the structure is more than increasing the stiffness of the structure.

The variations of the loss factor with the increase of the flexible core layer thickness to overall thickness ratio are presented in Figure 7. According to Figure 7, the loss factors decrease with the increase of the flexible core layer thickness to overall thickness ratio. Also, the variations of the loss factors in higher modes are less than those compared to the lower modes.

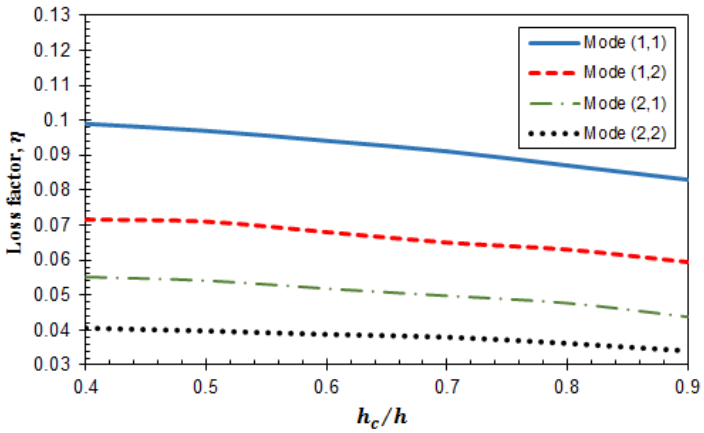


**Figure 7.** Effect of variations in the core layer thickness to overall thickness ratio on the loss factor

### Effect of the Foundation Parameters on the Natural Frequency

The effect of variations in the foundation parameters on the natural frequencies is presented in Table 4. The magnetic field intensity is considered 400 Guass and the other analysis conditions are similar to before. It can be realized from the results that the natural frequencies increase when $K_w$ and $K_g$ increase in each mode. The reason of these observations is that increasing the foundation parameters increases the foundation stiffness. Also, when the mode number increases, the increase in the natural frequency is obtained.

**Table 4.** Effect of the foundation parameters on the natural frequency and loss factor

| $K_w$ | $K_g = 0$ | | | | $K_g = 10^{15}$ | | | |
|---|---|---|---|---|---|---|---|---|
| | $\omega_{(1,1)}$ | $\omega_{(1,2)}$ | $\omega_{(2,1)}$ | $\omega_{(2,2)}$ | $\omega_{(1,1)}$ | $\omega_{(1,2)}$ | $\omega_{(2,1)}$ | $\omega_{(2,2)}$ |
| **0** | 2400.38 | 4595.79 | 5485.26 | 8287.99 | 2574.39 | 4754.35 | 5935.94 | 8509.13 |
| $\mathbf{10^5}$ | 2400.41 | 4596.79 | 5486.36 | 8302.99 | 2839.24 | 4909.14 | 6014.21 | 8536.11 |
| $\mathbf{10^{10}}$ | 2532.36 | 4715.91 | 5493.33 | 8473.06 | 2934.39 | 5022.31 | 6135.94 | 8609.14 |
| $\mathbf{10^{15}}$ | 2615.88 | 4755.40 | 5589.65 | 8644.03 | 3135.40 | 5254.37 | 6496.94 | 8699.86 |
| $\mathbf{10^{20}}$ | 2775.44 | 4856.02 | 5635.39 | 8719.18 | 3212.41 | 5356.02 | 6527.18 | 8769.34 |
| $\mathbf{10^{25}}$ | 2864.45 | 4856.02 | 5835.43 | 8749.22 | 3375.36 | 5521.12 | 6644.48 | 8821.51 |

## CONCLUSIONS

The free vibration analysis of a multi-layer rectangular plate with both MR fluid layers and a flexible core was presented while the plate was rested on a winkler-pasternak foundation. The applied theories for displacement fields in sheet layers and flexible core layer were exponential shear deformation theory and Frostig's second model, respectively. Hamilton's principle was used to solve the equations of motion and the Navier technique was used to solve them. It can be concluded from the obtained numerical results that the natural frequencies and loss factor increase with increasing magnetic field intensity. The increase in the MR layer thickness to overall thickness ratio causes the natural frequencies and loss factor decrease. Similarly, the increase in the core layer thickness to overall thickness ratio conduces the decrease in the natural frequencies and loss factors. The increase in the foundation parameters leads the increase in the natural frequencies.

## REFERENCES

[1] G. Iarriccio, A. Zippo, F. Pellicano, and M. Barbieri, "Resonances and nonlinear vibrations of circular cylindrical shells, effects of thermal gradients," *Proceedings of the Institution of Mechanical Engineers, Part C: Journal of Mechanical Engineering Science*, p. 0954406220907616, 2020.

[2] L. Benchouaf and E. H. Boutyour, "Nonlinear vibrations of buckled plates by an asymptotic numerical method," *Comptes Rendus Mécanique*, vol. 344, no. 3, pp. 151-166, 2016/03/01/ 2016.

[3] A. Nayak, S. Moy, and R. Shenoi, "Free vibration analysis of composite sandwich plates based on Reddy's higher-order theory," *Composites Part B: Engineering*, vol. 33, no. 7, pp. 505-519, 2002.

[4] J. Wang and G. Meng, "Magnetorheological fluid devices: principles, characteristics and applications in mechanical engineering," *Proceedings of the Institution of Mechanical Engineers, Part L: Journal of Materials: Design and Applications*, vol. 215, no. 3, pp. 165-174, 2001.

[5] K. D. Weiss, J. D. Carlson, and D. A. Nixon, "Viscoelastic properties of magneto-and electro-rheological fluids," *Journal of Intelligent Material Systems and Structures*, vol. 5, no. 6, pp. 772-775, 1994.

[6] X. Yao, C. Liu, H. Liang, H. Qin, Q. Yu, and C. Li, "Normal force of magnetorheological fluids with foam metal under oscillatory shear modes," *Journal of Magnetism and Magnetic Materials*, vol. 403, pp. 161-166, 2016.

[7] L. L. Yangbo YANG, Guang CHEN, Weihua LI, "Magnetorheological Properties of Aqueous Ferrofluids," *Nihon Reoroji Gakkaishi*, vol. 34, no. 1, pp. 25-31, 2006.

[8] X. Qiao *et al.*, "Magnetorheological Behavior of Polyethyene Glycol-Coated Fe3O4 Ferrofluids," *Nihon Reoroji Gakkaishi*, vol. 38, no. 1, pp. 23-30, 2010.

[9] Y.-Q. Guo, Z.-D. Xu, B.-B. Chen, C.-S. Ran, and W.-Y. Guo, "Preparation and experimental study of magnetorheological fluids for vibration control," *International Journal of Acoustics and Vibration*, vol. 22, no. 2, pp. 194-201, 2017.

[10] V. Rajamohan, V. Sundararaman, and B. Govindarajan, "Finite element vibration analysis of a magnetorheological fluid sandwich beam," *Procedia Engineering*, vol. 64, pp. 603-612, 2013.

[11] G. Bossis, O. Volkova, S. Lacis, and A. Meunier, "Magnetorheology: fluids, structures and rheology," in *Ferrofluids*: Springer, 2002, pp. 202-230.

[12] J. De Vicente, D. J. Klingenberg, and R. Hidalgo-Alvarez, "Magnetorheological fluids: a review," *Soft matter*, vol. 7, no. 8, pp. 3701-3710, 2011.

[13] E. Dragašius, V. Grigas, D. Mažeika, and A. Šulginas, "709. Evaluation of the resistance force of magnetorheological fluid damper," *Journal of Vibroengineering*, vol. 14, no. 1, 2012.

[14] H. Guo and W. Liao, "A novel multifunctional rotary actuator with magnetorheological fluid," *Smart Materials and Structures*, vol. 21, no. 6, p. 065012, 2012.

[15] D. J. Klingenberg, "Magnetorheology: Applications and challenges," *AIChE Journal*, vol. 47, no. 2, pp. 246-249, 2001.

[16] W. Li and H. Du, "Design and experimental evaluation of a magnetorheological brake," *The International Journal of Advanced Manufacturing Technology*, vol. 21, no. 7, pp. 508-515, 2003.

[17] H. Yamaguchi, X.-D. Niu, X.-J. Ye, M. Li, and Y. Iwamoto, "Dynamic rheological properties of viscoelastic magnetic fluids in uniform magnetic fields," *Journal of Magnetism and Magnetic Materials*, vol. 324, no. 20, pp. 3238-3244, 2012.

[18] Z.-F. Yeh and Y.-S. Shih, "Dynamic characteristics and dynamic instability of magnetorheological material-based adaptive beams," *Journal of Composite Materials*, vol. 40, no. 15, pp. 1333-1359, 2006.

[19] V. Rajamohan, S. Rakheja, and R. Sedaghati, "Vibration analysis of a partially treated multi-layer beam with magnetorheological fluid," *Journal of Sound and Vibration*, vol. 329, no. 17, pp. 3451-3469, 2010.

[20] F. Mohammadi and R. Sedaghati, "Nonlinear free vibration analysis of sandwich shell structures with a constrained electrorheological fluid layer," *Smart Materials and Structures*, vol. 21, no. 7, p. 075035, 2012.

[21] J.-Y. Yeh, "Vibration analysis of sandwich rectangular plates with magnetorheological elastomer damping treatment," *Smart Materials and Structures*, vol. 22, no. 3, p. 035010, 2013.

[22] J.-Y. Yeh, "Vibration characteristics analysis of orthotropic rectangular sandwich plate with magnetorheological elastomer," *Procedia Engineering*, vol. 79, pp. 378-385, 2014.

[23] M. Hoseinzadeh and J. Rezaeepazhand, "Vibration suppression of composite plates using smart electrorheological dampers," *International Journal of Mechanical Sciences*, vol. 84, pp. 31-40, 2014.

[24] M. Eshaghi, R. Sedaghati, and S. Rakheja, "Analytical and experimental free vibration analysis of multi-layer MR-fluid circular plates under varying magnetic flux," *Composite Structures*, vol. 157, pp. 78-86, 2016.

[25] G. Payganeh, K. Malekzadeh, and H. Malek-Mohammadi, "Free vibration of sandwich panels with smart magneto-rheological layers and flexible cores," *Journal of Solid Mechanics*, vol. 8, no. 1, pp. 12-30, 2016.

[26] M. Eshaghi, R. Sedaghati, and S. Rakheja, "Vibration analysis and optimal design of multi-layer plates partially treated with the MR fluid," *Mechanical Systems and Signal Processing*, vol. 82, pp. 80-102, 2017.

[27] A. G. Arani and T. Soleymani, "Size-dependent vibration analysis of a rotating MR sandwich beam with varying cross section in supersonic airflow," *International Journal of Mechanical Sciences*, vol. 151, pp. 288-299, 2019.

[28] E. Winkler, *Die Lehre von der Elasticitaet und Festigkeit: mit besonderer Rücksicht auf ihre Anwendung in der Technik für polytechnische Schulen, Bauakademien, Ingenieue, Maschinenbauer, Architecten, etc*. Dominicus, 1867.

[29] P. Pasternak, "Fundamentals of a new method of analyzing structures on an elastic foundation by means of two foundation moduli," *Proceedings of the Gosudarstvennoe Izdatelstro Liberaturi po Stroitelstvui Arkhitekture*, pp. 4-7, 1954.

[30] Z. Huang, C. Lü, and W. Chen, "Benchmark solutions for functionally graded thick plates resting on Winkler–Pasternak elastic foundations," *Composite Structures*, vol. 85, no. 2, pp. 95-104, 2008.

[31] H. A. Atmane, A. Tounsi, and I. Mechab, "Free vibration analysis of functionally graded plates resting on Winkler–Pasternak elastic foundations using a new shear deformation theory," *International Journal of Mechanics and Materials in Design*, vol. 6, no. 2, pp. 113-121, 2010.

[32] R. Benferhat, T. Hassaine Daouadji, and M. Said Mansour, "Free vibration analysis of FG plates resting on an elastic foundation and based on the neutral surface concept using higher-order shear deformation theory," *Comptes Rendus Mécanique*, vol. 344, no. 9, pp. 631-641, 2016/09/01/ 2016.

[33] K. Khorshidi and A. Fallah, "Buckling analysis of functionally graded rectangular nano-plate based on nonlocal exponential shear deformation theory," *International Journal of Mechanical Sciences*, vol. 113, pp. 94-104, 2016.

[34] Y. Frostig and O. T. Thomsen, "High-order free vibration of sandwich panels with a flexible core," *International Journal of Solids and Structures*, vol. 41, no. 5-6, pp. 1697-1724, 2004.

[35] J. N. Reddy, *Mechanics of laminated composite plates and shells: theory and analysis*. CRC press, 2004.

## NOMENCLATURE

| Parameter | Definition |
|---|---|
| $B$ | Magnetic field intensity |
| $E_1, E_2, E_3$ | Young's modulus in directions of layer material |
| $G_{12}, G_{1,3}, G_{2,3}$ | Shear modulus in directions of layer material |
| $G'$ and $G''$ | Storage modulus and loss modulus, respectively |
| $h$ | Thickness of the plate |
| $M_{xx}^i, M_{yy}^i, M_{xy}^i$ | Moment resultant for the $i^{th}$ layer |
| $M_{nxx}^c, M_{nyy}^c, M_{nxy}^c, M_{Qnxz}^c, M_{Qnyz}^c, M_z^c$ | Moment resultant for the flexible core layer |
| $N_{xx}^i, N_{yy}^i, N_{xy}^i, Q_{xz}^i, Q_{yz}^i$ | Force resultant for the $i^{th}$ layer |
| $R_z^c$ | Force resultant for the flexible core layer |
| $u, v, w$ | Displacement component in the x-, y-, and z-direction, respectively |

## GREEK SYMBOLS

| Parameter | Definition |
|---|---|
| $\varepsilon_{ij}$ | Strain on i-j plane |
| $\gamma_{ij}$ | Shearing strain on i-j plane |
| $\eta$ | Loss factor |
| $\nu_{12}, \nu_{1,3}, \nu_{2,3}$ | Poisson's ratio in directions of layer material |
| $\rho$ | Mass density per unit volume |
| $\varphi, \psi$ | Rotation components about the x- and y-direction, respectively |
| $\omega$ | Natural frequency |